J. Fluid Mech. (1979), *vol.* 93, *part* 2, *pp.* 305–317
Printed in Great Britain

Formation of a viscous boundary layer on the free surface of an imploding rotating liquid cylinder

By A. L. COOPER AND D. L. BOOK
Plasma Physics Division, Naval Research Laboratory,
Washington, D.C. 20375

(Received 23 March 1978)

The effect of viscosity on the inner free surface of a rotating imploding cylindrical liquid shell compressing an ideal gas or magnetic flux load is analysed in the limit of high Reynolds number Re. The condition of vanishing tangential stress on the free surface leads to the formation of a boundary layer of thickness $\sim Re^{-\frac{1}{2}}$. Within this layer the zonal velocity v is reduced by an amount Δv such that $\Delta v/v \sim Re^{-\frac{1}{2}}$. This results in a requirement of slightly increased rotation in order to satisfy the criterion for suppression of the Rayleigh–Taylor instability on the free surface. Calculations are presented for a model implosion trajectory.

1. Introduction

When a hollow rotating viscous incompressible fluid cylinder is imploded, the tangential shear stress distribution changes with time as a result of the competition between advection of angular momentum and viscous diffusion. If the radial implosion begins from a state of solid body rotation, viscous diffusion of angular momentum vanishes locally except for boundary effects which must diffuse from the solid boundaries or free surfaces which define the liquid cylinder. Implosions which are rapid on the scale of the viscous diffusion time can therefore be expected to display boundary layer character, with viscous effects concentrated within these layers. In regions far from the boundaries, angular momentum is conserved. The steady-state behaviour of viscous cylindrical rimming flows in a gravity field has been studied by Karweit & Corssin (1975), Ruschak & Scriven (1976) and Orr & Scriven (1978). Their results are to be contrasted with those of the present work in which we consider transient flows, in the absence of gravity, associated with an imploding cylindrical free surface.

Currently there is a great deal of interest in systems which achieve high energy densities through cylindrical implosions. Examples are axial flux compression experiments, surveyed by Knoepfel (1970), attempts to induce the transition to the metallic state in hydrogen (Grivorev *et al.* 1972), and concepts for the production of thermonuclear plasmas using solid (Alikhanov *et al.* 1977) or liquid (Book *et al.* 1977) metal shells (liners). This last is at present the subject of an experimental programme at the Naval Research Laboratory.

A distinctive feature of the devices employed in the NRL experiments is that they are designed to implode and rebound stably, in a repetitive fashion. To achieve this it is necessary to forestall the development of the Rayleigh–Taylor instability at both the inner and outer surfaces of the liner. The inner free surface can be stabilized

0022–1120/79/4195–6170 $02.00

throughout the entire liner trajectory by imposing sufficient rotation about the cylinder axis, which introduces a centripetal acceleration opposing $\ddot{R}$, while the outer surface remains in contact with a set of axial or radial pistons driven by high pressure gas. This combination of rotation and hydraulic piston implosion leads to liners which are theoretically stable against Rayleigh–Taylor modes.

While rotational stabilization of the inner free surface has been demonstrated theoretically by Barcilon, Book & Cooper (1974) for an ideal inviscid liner and established experimentally (Turchi *et al.* 1976; Burton *et al.* 1977), the precise role of real liner fluid viscosity has remained an open question. In this paper we study the effects of liner viscosity on the motion of a cylindrical rotating imploding liner in the realistic limit of large Reynolds number (experimental Reynolds numbers Re of the order of 2×10^4 typical). We find that viscous effects are concentrated in a thin boundary layer at the free surface whose thickness is of the order of $Re^{-\frac{1}{2}}$. The bulk of the liner behaves essentially inviscidly. Within the viscous boundary layer, the rotational speed of the liner at the free surface is reduced from that which would occur inviscidly. The boundary layer thickness and reduction in angular velocity are determined as quadratures of the basic state trajectory, $R(t)$. Numerical results are obtained for a prescribed model radial trajectory and presented as a function of the compression ratio and Reynolds number.

2. Analytical treatment

The liquid liner is assumed to undergo a flow in the r, ϕ plane corresponding to the motion of an infinite hollow cylinder which is imploding while rotating about its axis. Rotation is necessary both for the initial formation of the liner and to stabilize against the Rayleigh–Taylor instabilities near the inner turning point. In this study we will concentrate on the inner free surface and, without any essential restriction in the physics, will consider the liner to be infinitely thick.

The following assumptions are made:

(1) The liner is launched from a state of rigid rotation with angular velocity Ω_0 at time $t = 0$.

(2) The liner is incompressible (constant density ρ).

(3) The liner kinematic viscosity ν is constant,

(4) The flow is laminar.

(5) The flow is one-dimensional $\left(\dfrac{\partial}{\partial \phi} = \dfrac{\partial}{\partial z} = 0\right)$.

(6) Surface tension is neglected.

Incompressibility of the liner in this case implies

$$\partial(ru)/\partial r = 0. \tag{1}$$

where $u(r,t)$ is the radial velocity component. The radial component of the Navier–Stokes equation governs the radial motion,

$$\frac{\partial u}{\partial t} + u\frac{\partial u}{\partial r} - \frac{v^2}{r} + \frac{1}{\rho}\frac{\partial p}{\partial r} = \nu \frac{\partial}{\partial r}\left[\frac{1}{r}\frac{\partial}{\partial r}(ru)\right], \tag{2}$$

where $v(r,t)$ is the zonal velocity and $p(r,t)$ is the pressure. The angular momentum

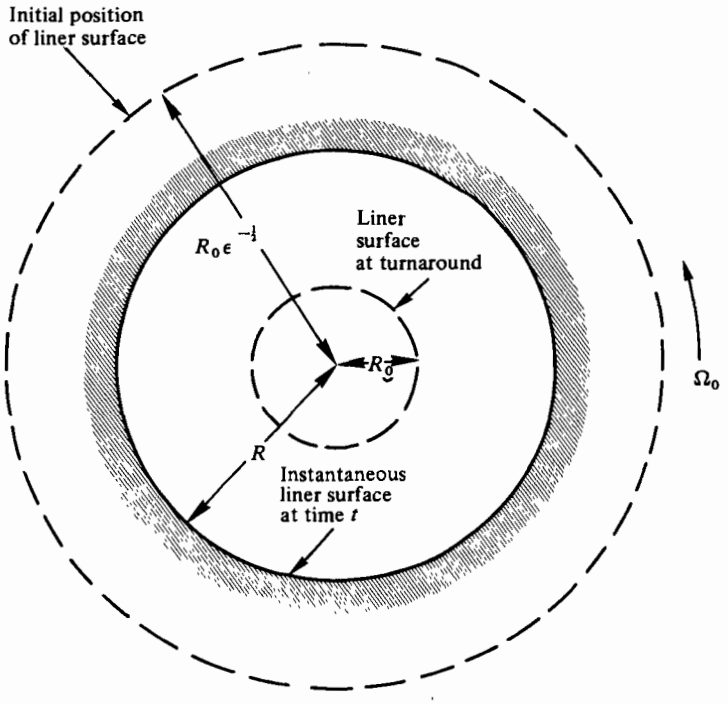

FIGURE 1. Geometry of the model used to study viscous effects at the free surface of a rotating imploding liner.

equation, which is formed from the zonal component of the Navier–Stokes equation, is given as

$$\frac{\partial(rv)}{\partial t} + u\frac{\partial}{\partial r}(rv) = \nu r\frac{\partial}{\partial r}\left[\frac{1}{r}\frac{\partial}{\partial r}(rv)\right]. \tag{3}$$

Substitution of (1) into (2) reveals that the right-hand side of the radial momentum equation vanishes. Viscous effects on the radial motion arise only through coupling with the zonal momentum equation (3) by virtue of the centripetal acceleration term $-v^2/r$. An additional viscous effect arises at the free surface, where the normal stress is balanced. This will be discussed later in the paper when we consider the boundary conditions.

The coupled equations (1)–(3) should be solved consistent with proper initial and boundary conditions to obtain $u(r,t)$, $v(r,t)$ and $p(r,t)$. In order to emphasize the main physics of this problem in its most simple form, we will instead consider the radial trajectory of the liner to be prescribed, and generate consistent solutions to the angular momentum equation. The viscous evolution of the angular momentum distribution is direct, while the viscous effects upon the radial velocity field are mainly a result of the coupling to the zonal equation through the centripetal acceleration term.

(*A*) *Radial trajectory*

We therefore consider a prescribed radial trajectory defined by the motion of the free surface radius

$$R = R(t/t_0;\epsilon), \tag{4}$$

where t_0, the hydrodynamic time, is characteristic of the throw time (time required to go from the initial radius $R_0\epsilon^{-\frac{1}{2}}$ to the minimum radius R_0), and $\epsilon^{\frac{1}{2}}$ represents the ratio of minimum to maximum radius (compression ratio). These dimensions and parameters are indicated in figure 1.

Integrating the continuity equation (1) we obtain

$$ru = R\,dR/dt = K(t), \tag{5}$$

i.e. ru is a constant throughout the liner at any given time t. Therefore, the specification of the free surface trajectory, (4), completely defines the entire radial velocity field of the liner.

(*B*) *Initial and boundary conditions*

We desire a solution to (3) with the prescribed trajectory given by (4). Since the liner is launched from a rigid rotation state with angular velocity Ω_0, the initial condition on the angular momentum $a(r,t) = rv$ is

$$a(r,0) = r^2\Omega_0, r \geqslant R_0\epsilon^{-\frac{1}{2}}. \tag{6}$$

A suitable boundary condition must also be applied at the free surface, $r = R(t)$. The free surface is an interface between the liquid and a gas, magnetic field or magnetic field-plasma mixture. In any case, there should be negligible tangential shear stress $\sigma_{r\phi}$ at the free surface, and the normal stress in the liquid liner should be in balance with the material and/or magnetic pressure p of the interior volume there. Therefore at the interface,

$$\sigma_{r\phi} = \rho\nu r\frac{\partial}{\partial r}\left(\frac{a}{r^2}\right) = 0; \tag{7}$$

$$p - 2\nu\rho\,\partial u/\partial r = p_i. \tag{8}$$

The vanishing of the tangential shear stress prescribed by (7) implies that at $r = R(t)$ the angular momentum satisfies

$$a = Cr^2. \tag{9}$$

Thus the zonal velocity field is locally that of a rigid-body rotation with arbitrary angular velocity given by the integration constant C, which is in general a function of time.

We notice that the boundary condition, (7), is satisfied by the initial condition, (6), which specifies that the liner is launched from a state of rigid rotation.

Equations (6) and (7) provide one initial condition and one boundary condition for the angular momentum equation, (3). An additional boundary condition is required since we have a second-order partial differential equation in r. This second boundary condition arises as a far-field condition in the liner for $r > R$. To see this more clearly, we observe that the inviscid solution ($\nu = 0$) of (3), subject to the initial condition, (6), satisfies the full viscous equation, but not the boundary condition, (7). We therefore anticipate that far from the free surface, $r \gg R$, the liner will behave inviscidly. A viscous boundary layer will exist at the free surface which recovers the boundary condition, (7), at the free surface and matches with the inviscid solution in the interior of the liner. This matching condition provides the second required boundary condition.

Figure 2 illustrates the nature of this viscous boundary layer. The liner is shown launched at time $t = 0$ with a solid-body rotation Ω_0 corresponding to that of the

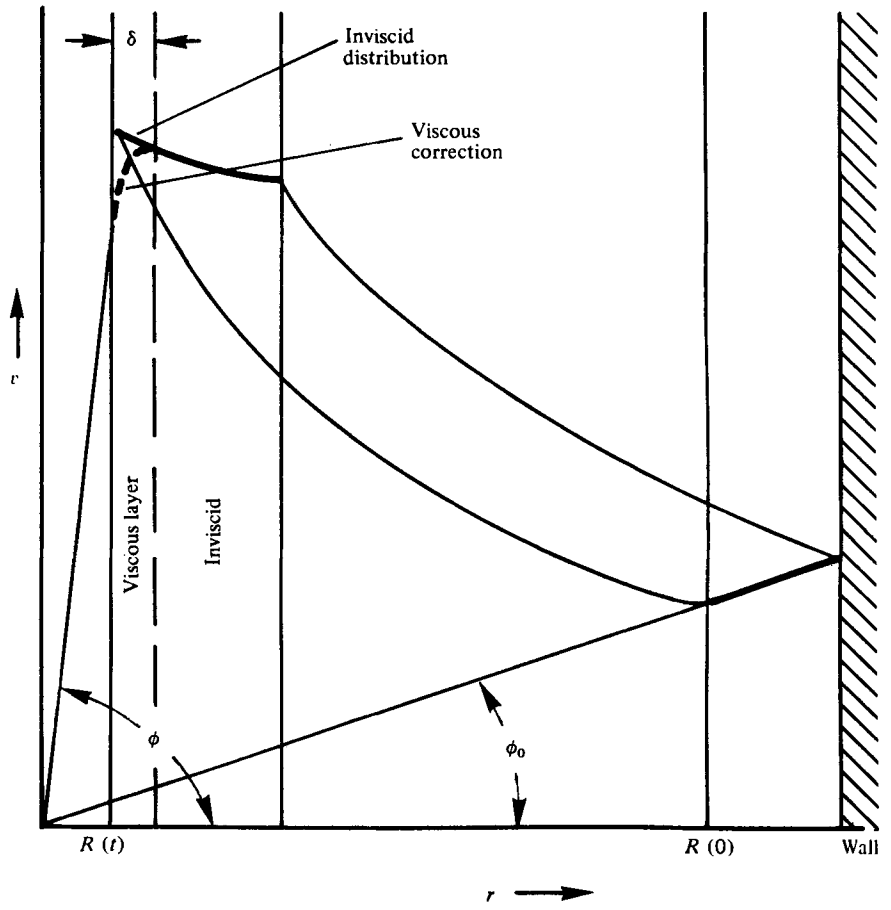

FIGURE 2. Schematic representation of the viscous boundary layer at the free surface of the liner, showing the reduction in surface zonal velocity resulting from the condition of zero tangential shear stress. $\Omega = \tan\phi$ and $\Omega_0 = \tan\phi_0$.

apparatus. The liner is also depicted at a later time t, after it has imploded to a radius $R(t)$. The inviscid zonal velocity variation appropriate at that time is indicated by the solid line. This variation corresponds to conservation of specific angular momentum rv for each of the fluid lamellae composing the liner. The viscous layer or boundary layer correction is shown in the region δ by means of the dashed line. The viscous solution satisfies the stressless condition at the surface and matches with the inviscid distribution in the interior. Viscosity is seen to slow down the liner interface zonal velocity. This is important, as we rely on the strong zonal motion of the inside surface in the vicinity of the turning point to stabilize against Rayleigh–Taylor instabilities.

(*C*) *Lagrangian variables*

Because of the motion of the free surface and the inherent competition between convection with geometric convergence and diffusion displayed in (3), it is more convenient to transform to Lagrangian variables. We therefore take

$$\xi = r^2 - R^2(t), \tag{10}$$

which is proportional to the displaced area relative to the moving interface and is conserved for fluid shells in an incompressible liner. This transformation has been used previously in a related problem by Cooper & Book (1978).

The angular momentum equation for $a = A(\xi, t)$ becomes

$$\frac{\partial A}{\partial t} = 4\nu[R^2(t) + \xi]\frac{\partial^2 A}{\partial \xi^2}, \tag{11}$$

with initial and boundary conditions

$$A(\xi, 0) = [R^2(0) + \xi]\,\Omega_0, \tag{12}$$

$$\frac{\partial A}{\partial \xi}(0, t) = \frac{A(0, t)}{R^2(t)}, \tag{13}$$

and for $\xi \to \infty$, $$A(\xi, t) \sim [\xi + R^2(0)]\,\Omega_0. \tag{14}$$

Equation (14) requires that the solution match with the inviscid solution far into the liner.

(D) *Non-dimensionalization*

The dependent and independent variables are normalized as follows:

$$\tilde{A} = A/R_0^2\,\Omega_0, \quad \tilde{t} = t/t_0, \quad \tilde{R} = R/R_0, \quad \tilde{\xi} = \xi/R_0^2.$$

Two dimensionless parameters characterize the problem:

$$\epsilon = R_0^2/R^2(0), \quad Re = R_0^2/4\nu t_0. \tag{16), (17}$$

Re, a Reynolds number, represents the ratio of the diffusion time $R_0^2/4\nu$ to the hydrodynamic time associated with the prescribed radial motion, t_0. Since this is a boundary layer problem, we anticipate that the viscous zone will scale as $Re^{-\frac{1}{2}}$. As previously defined, ϵ is an inverse compression ratio representing the ratio of the final compression area to its initial value for the prescribed trajectory. In terms of these non-dimensional variables, the relevant equations and initial and boundary conditions become

$$\partial\tilde{A}/\partial\tilde{t} = Re^{-1}[\tilde{R}^2(\tilde{t}) + \tilde{\xi}]\,\partial^2\tilde{A}/\partial\tilde{\xi}^2, \tag{18}$$

$$\tilde{A}(\tilde{\xi}, 0) = \tilde{\xi} + 1/\epsilon, \tag{19}$$

$$\partial\tilde{A}(0, \tilde{t})/\partial\tilde{\xi} = \tilde{A}(0, \tilde{t})/\tilde{R}^2(\tilde{t}) \tag{20}$$

and $$\tilde{A}(\tilde{\xi}, \tilde{t}) \sim \tilde{\xi} + 1/\epsilon \tag{21}$$

at large $\tilde{\xi}$. Here $\tilde{R}(\tilde{t})$ describes the liner trajectory, which may be either measured or calculated. For a given $\tilde{R}(\tilde{t})$, finding a solution to (18)–(21) valid throughout Re–ϵ parameter space represents a formidable task. For large values of Re, the situation is significantly simplified. This limit is also of practical interest, as the Reynolds numbers associated with magnetic compression using liquid metal liners are of the order of 2×10^4.

(E) *Asymptotic theory at large Reynolds number*

We concentrate on the large-Reynolds-number portion of the Re–ϵ parameter space. In particular, we seek the behaviour of (18)–(21) in the following asymptotic limit:

$$Re^{-\frac{1}{2}} \ll 1, \tag{22}$$

and will apply the methods of matched asymptotic analysis to (18)–(21), taking advantage of the small parameter $Re^{-\frac{1}{2}}$. Henceforth, we omit the tilde from dependent and independent variables, with the understanding that all variables are dimensionless.

(*a*) *Outer solution.* We expand the angular momentum A in a regular perturbation expansion in terms of the small parameter $Re^{-\frac{1}{2}}$.

$$A(\xi,t;Re,\epsilon) \sim A^{(0)}(\xi,t;\epsilon)+Re^{-\frac{1}{2}}A^{(1)}(\xi,t;\epsilon)+\dots. \tag{23}$$

To lowest order in $Re^{-\frac{1}{2}}$, (18)–(21) become

$$\partial A^{(0)}/\partial t = 0, \tag{24}$$

with

$$A^{(0)}(\xi,0) = \xi+1/\epsilon, \tag{25}$$

$$\partial A^{(0)}/\partial\xi(0,t) = A^{(0)}/R^2(t), \tag{26}$$

and

$$A^{(0)}(\xi,t) \sim \xi+1/\epsilon \tag{27}$$

at large ξ. The solution to (24) which satisfies (25) and (27) is

$$A^{(0)}(\xi,t;\epsilon) = \xi+1/\epsilon. \tag{28}$$

This solution does not, however, satisfy the required stressless boundary condition, (26). We therefore have the ingredients for a classical boundary layer. It is necessary to rescale the independent variable ξ to recover the missing boundary condition and resolve this layer.

(*b*) *Inner solution.* The necessary stretching of ξ is given as

$$\eta = Re^{\frac{1}{2}}\xi, \tag{29}$$

and the dependent variable is written as

$$\hat{A} = \hat{A}(\eta,t;\epsilon). \tag{30}$$

In terms of (29) and (30), the governing equations, (18)–(21), become

$$\frac{\partial\hat{A}}{\partial t} = [R^2(t)+\eta Re^{-\frac{1}{2}}]\frac{\partial^2\hat{A}}{\partial\eta^2}, \tag{31}$$

$$\hat{A}(\eta,0) = 1/\epsilon+\eta Re^{-\frac{1}{2}}, \tag{32}$$

$$\frac{\partial\hat{A}}{\partial\eta}(0,t) = Re^{-\frac{1}{2}}\frac{\hat{A}(0,t)}{R^2(t)}, \tag{33}$$

$$\hat{A}(\eta,t) \sim 1/\epsilon+\eta Re^{-\frac{1}{2}}, \quad \eta \gg 1. \tag{34}$$

The initial and boundary conditions satisfied by (32) and (34) are evidently the inner representation of the inviscid outer solution and satisfy the differential equation, (31). It is therefore convenient to define a new angular momentum variable by means of

$$\bar{A}(\eta,t;\epsilon) = \hat{A}(\eta,t;\epsilon)-(1/\epsilon+\eta Re^{-\frac{1}{2}}). \tag{35}$$

$\bar{A}(\eta,t;\epsilon)$ represents the viscous correction to the solution. Equations (31)–(34) become

$$\frac{\partial\bar{A}}{\partial t} = [R^2(t)+\eta Re^{-\frac{1}{2}}]\frac{\partial^2\bar{A}}{\partial\eta^2}, \tag{36}$$

with

$$\bar{A}(\eta, 0) = 0, \tag{37}$$

$$\frac{\partial \bar{A}}{\partial \eta}(0,t) = Re^{-\frac{1}{2}}\left[\frac{\bar{A}(0,t)+1/\epsilon}{R^2(t)} - 1\right], \tag{38}$$

and

$$\lim_{\eta\to\infty} \bar{A}(\eta, t) = 0. \tag{39}$$

We now expand $\bar{A}$ as a regular perturbation expansion in powers of the small parameter $Re^{-\frac{1}{2}}$.

$$\bar{A}(\eta, t; Re, \epsilon) \sim \bar{A}^{(0)}(\eta, t; \epsilon) + Re^{-\frac{1}{2}}\bar{A}^{(1)}(\eta, t; \epsilon) + \ldots. \tag{40}$$

To lowest order in $Re^{-\frac{1}{2}}$ we find that

$$\bar{A}^{(0)} = 0, \tag{41}$$

and to next order we obtain

$$\partial \bar{A}^{(1)}/\partial t = R^2(t)\,\partial^2 \bar{A}^{(1)}/\partial \eta^2 \tag{42}$$

with

$$\bar{A}^{(1)}(\eta, 0) = 0, \tag{43}$$

$$\frac{\partial \bar{A}^{(1)}}{\partial \eta}(0,t) = 1/[\epsilon R^2(t)] - 1, \tag{44}$$

and

$$\lim_{\eta\to\infty} \bar{A}^{(1)}(\eta, t) = 0. \tag{45}$$

Defining a new timelike variable, the age,

$$\theta = \int_0^t R^2(t')\,dt', \tag{46}$$

reduces (42) to a diffusion equation which is identical to that governing diffusion in a slab,

$$\partial \bar{A}^{(1)}/\partial \theta = \partial^2 \bar{A}^{(1)}/\partial \eta^2. \tag{47}$$

It should be borne in mind that η is a dimensionless area and θ is a stretched time variable which is weighted over the trajectory. That is, even though (47) has the form of a slab diffusion, it still includes effects of geometric convergence consistent with the liner motion asymptotically correctly for the large Reynolds number limit considered here.

The solution to (47) with the conditions of (43)–(45) is written as

$$\bar{A}^{(1)}(\eta, \theta; \epsilon) = -\frac{1}{\pi^{\frac{1}{2}}}\int_0^\theta \frac{d\tau e^{-\eta^2/4(\theta-\tau)}}{(\theta-\tau)^{\frac{1}{2}}}\,[1/\epsilon R^2(\tau) - 1]. \tag{48}$$

Equation (48), the viscous correction to the angular momentum, is given as a quadrature over the basic state trajectory $R(\tau)$. That is, $\bar{A}^{(1)}$ is a function not only of the compression ratio ϵ, but of the details of the full trajectory in terms of the age defined in (46).

Thus the angular momentum distribution is from (35) and (48)

$$\hat{A}(\eta, t; Re, \epsilon) \sim \left(\frac{1}{\epsilon} + \eta Re^{-\frac{1}{2}}\right)$$

$$- Re^{-\frac{1}{2}}\frac{1}{\pi^{\frac{1}{2}}}\int_0^\theta \frac{d\tau e^{-\eta^2/4(\theta-\tau)}}{(\theta-\tau)^{\frac{1}{2}}}\,(1/\epsilon R^2 - 1). \tag{49}$$

Of particular interest is the angular momentum at the free surface. This is basic to stabilization of the Rayleigh–Taylor instability which could occur near the inner turning point $t = t_0$. Taking $\eta \to 0$ we find

$$\hat{A}(0,t;Re,\epsilon) \sim \frac{1}{\epsilon} - Re^{-\frac{1}{2}} \frac{1}{\pi^{\frac{1}{2}}} \int_0^\theta \frac{d\tau}{(\theta-\tau)^{\frac{1}{2}}} \left[\frac{1}{\epsilon R^2(\tau)} - 1\right]. \tag{50}$$

Therefore, the angular velocity of the free surface is given as

$$\frac{\Omega}{\Omega_0} = \frac{1}{R^2(\theta)} \left\{\frac{1}{\epsilon} - Re^{-\frac{1}{2}} \frac{1}{\pi^{\frac{1}{2}}} \int_0^\theta \frac{d\tau}{(\theta-\tau)^{\frac{1}{2}}} \left[\frac{1}{\epsilon R^2(\tau)} - 1\right]\right\}, \tag{51}$$

or

$$\frac{\Omega}{\Omega_{\text{inv}}} = 1 - Re^{-\frac{1}{2}} \epsilon \frac{1}{\pi^{\frac{1}{2}}} \int_0^\theta \frac{d\tau}{(\theta-\tau)^{\frac{1}{2}}} \left[\frac{1}{\epsilon R^2(\tau)} - 1\right] \equiv 1 - Re^{-\frac{1}{2}} f(t,\epsilon), \tag{52}$$

where $\Omega_{\text{inv}} = \Omega_0/\epsilon R^2$ is the inviscid surface angular velocity. The reduction in angular velocity of the free surface from its inviscid value is seen to scale as $Re^{-\frac{1}{2}}$.

We next investigate the question of the uniform validity of our asymptotic analysis. Since (47) is in the form of a semi-infinite slab diffusion problem with homogeneous initial and boundary conditions at infinity, the solution represented by (48) displays viscous effects concentrated in a boundary region whose effective thickness scales as

$$\langle\eta\rangle \sim [\theta(t)]^{\frac{1}{2}}. \tag{53}$$

Therefore, we see that the higher order curvature term in (36) will provide a correction which scales as

$$\eta Re^{-\frac{1}{2}} \sim (\theta/Re)^{\frac{1}{2}}. \tag{54}$$

Comparing this term to $R^2(t)$, the term retained in lowest order in (36), we find the condition for uniform validity of the lowest order asymptotic expansion

$$(\theta(t)/Re)^{\frac{1}{2}} \ll R^2(t). \tag{55}$$

This condition is most stringent at turnaround, $t = 1$, where $R^2(t)$ is minimum. There it takes the form

$$\theta^{\frac{1}{2}}(1,\epsilon) \ll Re^{\frac{1}{2}}. \tag{56}$$

This provides a restriction on the magnitude of ϵ as a function of Re for uniform validity of the asymptotic analysis. The age θ, defined by (46) as a time integral over the basic trajectory $R^2(t)$ is a function of both t and ϵ. $R^2(t)$ varies from ϵ^{-1} to 1 as t varies from 0 to 1. Therefore,

$$1 \leqslant \int_0^t R^2(t)\,dt = \theta \leqslant \epsilon^{-1}. \tag{57}$$

By (56) and (57) we see that as a maximum constraint on ϵ we have

$$\epsilon \gg Re^{-1}. \tag{58}$$

For trajectories which are sufficiently flat near turnaround this restriction on ϵ is overly severe, and our results should remain valid for arbitrary $\epsilon < 1$. Physically, the restriction on ϵ is to ensure that the boundary layer thickness remains small compared with the instantaneous free surface radius.

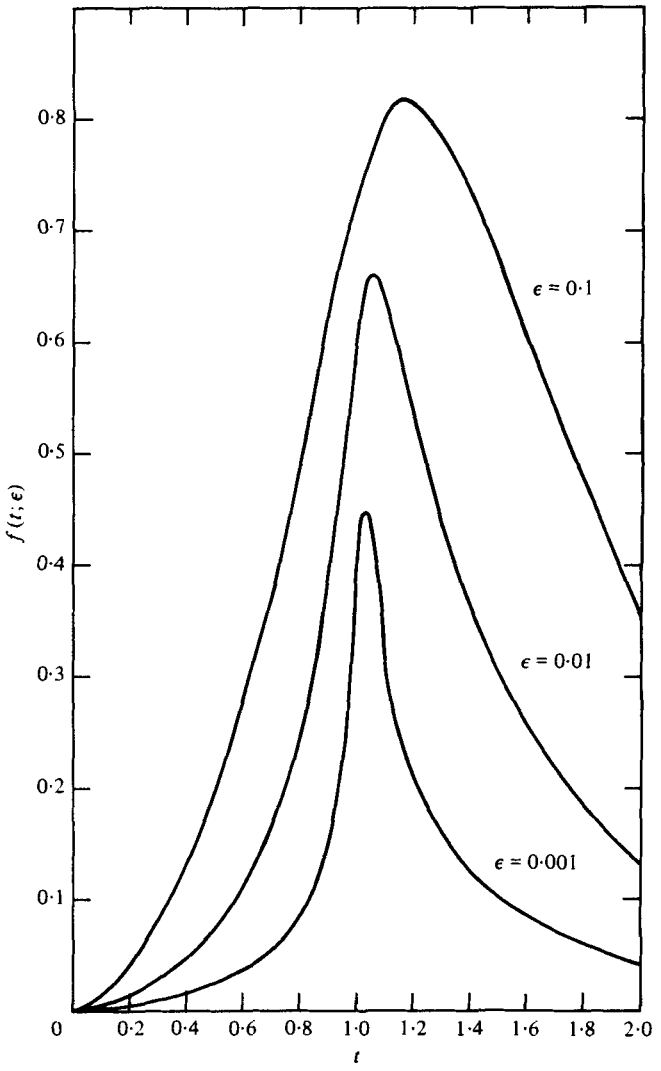

FIGURE 3. Coefficient of the viscous correction to surface zonal velocity *vs.* time for various compression ratios.

3. Numerical results

In this section, the general formulas derived in the previous section are specialized to a particular prescribed liner trajectory and the results of evaluating the required quadratures are discussed. Special emphasis is placed on the viscous perturbation of the free-surface angular velocity, since this quantity is most important in ensuring stable and well controlled liner implosions. We consider a 'parabolic' trajectory

$$R^2(t;\epsilon) = 1 + (1/\epsilon - 1)(1-t)^2. \tag{59}$$

It can be shown that this type of trajectory represents a realistic limit of a *thin* freely launched liner, $\Delta/R \ll 1$, where Δ is the liner thickness. The numerical results to be presented in this study will be associated with this trajectory. For strict consistency

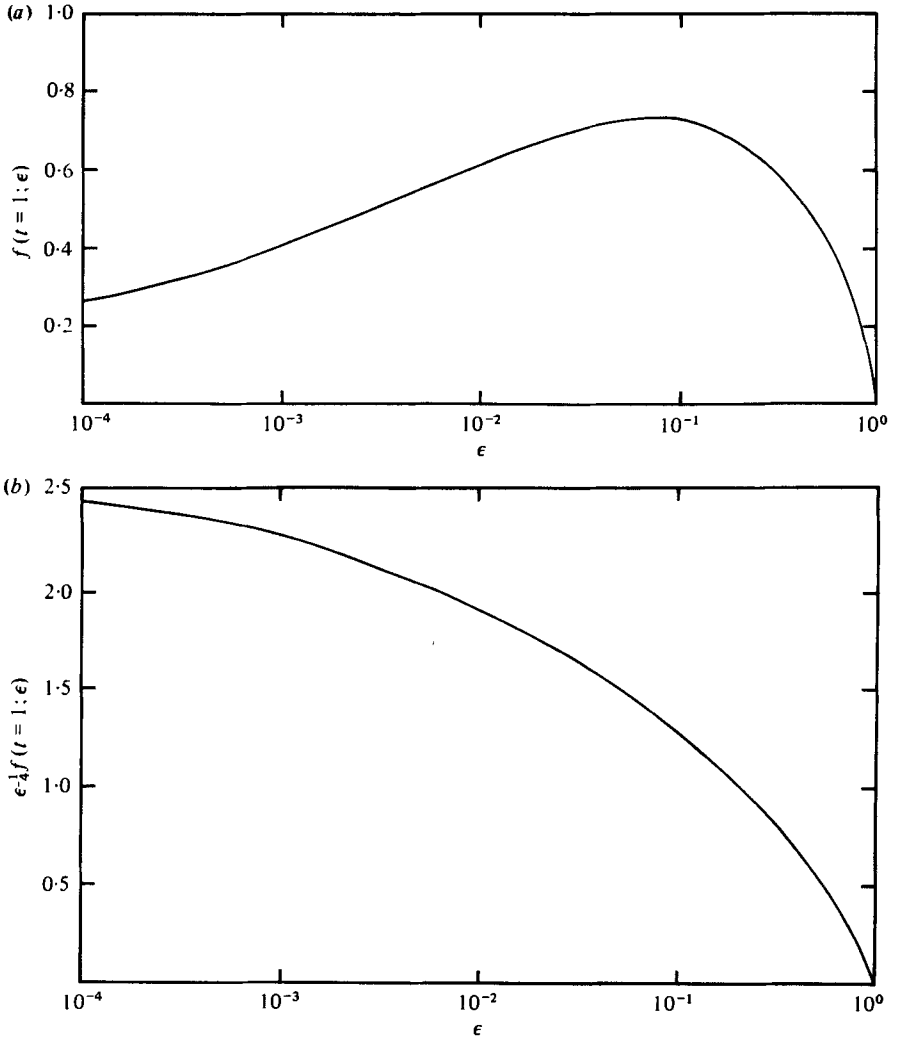

FIGURE 4. (*a*) Plot of the viscous correction coefficient [equation (52)] at turnaround $f(1;\epsilon)$ *vs.* ϵ. (*b*) Plot of $\epsilon^{-\frac{1}{4}}f(1;\epsilon)$, showing the asymptotic behaviour $f(1;\epsilon) \sim \epsilon^{\frac{1}{4}}$ at small ϵ.

with our previous approximation that the outer radius is at infinity, it is necessary that viscous effects be confined to a layer of thickness $\delta \ll \Delta$.

The integral in (52) was evaluated numerically. The integration variable was taken to be t instead of θ, using the transformation $d\theta = dt(d\theta/dt)$ and evaluating $d\theta/dt$ by (46). Dividing the range of integration into 10^4 equal-time intervals and using the trapezoid rule yielded results accurate to $\sim 1\%$. Landen's transformation (Abramowitz & Stegun 1970, p. 597) was used to evaluate the incomplete elliptic integral which results when parabolic trajectories [equation (59)] are employed in (52).

In figure 3, the viscous correction to the free surface angular velocity, f, as defined in (52), is plotted as a function of time for various values of ϵ. The viscous reduction in surface angular velocity is seen to evolve from zero at $t = 0$ and increase with time, slowly at first, and then rapidly near the inner turning point, $t = 1$. The maximum value, of order 1 in all cases, is obtained shortly after the turning point for this model

trajectory. As the liner moves outward toward its maximum radius at $t = 2$, the correction decreases. The correction does not vanish entirely, however, even at $t = 2$ when the liner has returned to its initial radius. Figure 3 shows that there is significant ϵ dependence in the effects produced by finite viscosity. In particular, we see that f tends to decrease as $\epsilon \to 0$. It can be shown in this limit that for $t \neq 1$,

$$f(t;\epsilon) \sim \epsilon^{\frac{1}{2}}, \tag{60}$$

while at $t = 1$

$$f(1;\epsilon) \sim \epsilon^{\frac{1}{4}}, \tag{61}$$

provided inequality (58) continues to hold.

At turnaround, $t = 1$, where rotational stabilization is most critical,

$$\lim_{\epsilon \to 0} \epsilon^{-\frac{1}{4}} f(1;\epsilon) = 2{\cdot}44. \tag{62}$$

Therefore from (52), at $t = 1$,

$$(\Omega_{\text{inv}} - \Omega)/\Omega_{\text{inv}} \simeq 2{\cdot}44 Re^{-\frac{1}{4}} \epsilon^{\frac{1}{4}} = 2{\cdot}44 (Re)_{\text{eff}}^{-\frac{1}{2}}, \tag{63}$$

where

$$(Re)_{\text{eff}} = R_0 R_{\max}/4\nu t_0 \tag{64}$$

is an effective Reynolds number related to both the minimum (R_0) and maximum ($R_{\max}$) radii of the trajectory.

But it is also clear that

$$\lim_{\epsilon \to 1} f(t;\epsilon) = 0. \tag{65}$$

The behaviour in both limits is shown in figure 4(*a*), where we plot the surface angular velocity correction at $t = 1$ as a function of ϵ. Figure 4(*b*) shows the same curve, scaled by $\epsilon^{-\frac{1}{4}}$ to exhibit the asymptotic dependence of (61).

For liquid alkali metals, a typical viscosity is $\nu \simeq 10^{-2}$ cm^2/s. Taking $t_0 \simeq 10^{-3}$ s, $R_0 = 1$ cm and $\epsilon = 10^{-3}$ yields $(Re)_{\text{eff}}^{-\frac{1}{2}} \simeq 10^{-3}$. Thus the relative change in surface angular velocity due to viscous effects is always less than one per cent in cases of practical interest.

4. Summary

Viscous effects for imploding liners at large ratios of viscous diffusion time to hydrodynamic time (high Reynolds number) are confined to thin boundary layers near the stressless free surface. The boundary layer thickness scales as $Re^{-\frac{1}{2}}$, with the interior region of the liner behaving inviscidly. The resulting problem has been solved by the methods of matched asymptotic analysis. A boundary layer structure has been obtained which satisfies an equation identical to those associated with one-dimensional slab diffusion while properly including the effects of geometrical convergence. The results obtained indicate that the free surface angular momentum is reduced from its inviscid value by an amount proportional to $Re^{-\frac{1}{2}}$.

This work was supported by the U.S. Department of Energy and the U.S. Office of Naval Research.

REFERENCES

ABRAMOWITZ, M. & STEGUN, I. (ed.) 1970 *Handbook of Mathematical Functions*. Dover.

ALIKHANOV, S. G., BAKHTIN, V. P., BRUSNIKIN, V. M., GLUSHKOV, I. S., KURTMULLAEV, R. Kh., LUMIN, A. L., MAZYCHENKO, A. D., NORIKOV, V. P., PICHYGIN, V. V., SEMENOV, V. N., SMOLKIN, G. E., UTYUGOV, E. G. & SHIPUK, I. Ya. 1977 Study of models of liner thermonuclear systems. *Plasma Phys. Controlled Nucl. Fusion Res.* 1976, vol. 3, pp. 517–526. Int. Atomic Energy Authority.

BARCILON, A., BOOK, D. L. & COOPER, A. L. 1974 Hydrodynamic stability of a rotating liner, *Phys. Fluids* **17**, 1707–1718.

BOOK, D. L., COOPER, A. L., FORD, R., HAMMER, D., JENKINS, D. J., ROBSON, A. E. & TURCHI P. J. 1977 Stabilized imploding liner fusion systems. *Plasma Phys. Controlled Nucl. Fusion Res.* 1976, vol. 3, pp. 507–516. Int. Atomic Energy Authority.

BURTON, R. L., TURCHI, P. J., JENKINS, D. J. & COOPER, A. L. 1977 Hydrodynamic model experiments for stabilized liquid liner with annular piston drive. *Proc. 7th Symp. Engng Problems of Fusion Res., Knoxville, Tennessee*, pp. 225–230.

COOPER, A. L. & BOOK, D. L. 1978 Magnetic flux diffusion in imploding liquid liners. *Phys. Fluids* **21**, 34–41.

GRIVOREV, F. V., KORMER, S. B., MIKHAILOVA, O. L., TOLOCHKO, A. P. & URLIN, V. D. 1972 Experimental determination of the compressibility of hydrogen at densities 0·5–2 g/cm^3. Metallization of hydrogen. *Zh. Eksp. Teor. Fiz. Pisma Red.* **16**, 286–290 [*Sov. Phys. J. Exp. Theor. Phys. Lett.* **16**, 201–204].

KARWEIT, M. J. & CORRSIN, S. 1975 Observations of cellular pattern in a partly filled, horizontal rotating cylinder. *Phys. Fluids* **18**, 111–112.

KNOEPFEL, H. 1970 *Pulsed High Magnetic Fields*. North Holland.

ORR, F. M. & SCRIVEN, L. E. 1978 Rimming flow: numerical simulation of steady, viscous, free-surface flow with surface tension. *J. Fluid Mech.* **84**, 145–165.

RUSCHAK, K. J. & SCRIVEN, L. E. 1976 Rimming flow of liquid in a rotating horizontal cylinder *J. Fluid Mech.* **76**, 113–125.

TURCHI, P. J., COOPER, A. L., FORD, R. & JENKINS, D. L. 1976 Rotational stabilization of an imploding liquid cylinder. *Phys. Rev. Lett.* **36**, 1546–1549.